JANNER, A. & JANSSEN, T. (1979). *Physica (Utrecht)*, **99A**, 47-76.
JANNER, A., JANSSEN, T. & DE WOLFF, P. M. (1983). *Acta Cryst.* **A39**, 658-666.
KUCHARCZYK, D., PACIOREK, U. A. & USZYNSKI, I. J. A. (1986). Abstr. Proc. Int. Conf. on Polytypes and Modulated Structures, Wrocław, Poland, p. 79.
LEUNG, P. C. W., EMGE, T. J., BENO, M. A., WANG, H. H., WILLIAMS, J. M., PETŘÍČEK, V. & COPPENS, P. (1985). *J. Am. Chem. Soc.* **107**, 6184-6191.
PEREZ-MATO, J. M., MADARIAGA, G. & TELLO, M. J. (1986). *J. Phys. C*, **19**, 2613-2622.
PETŘÍČEK, V., COPPENS, P. & BECKER, P. (1985). *Acta Cryst.* **A41**, 478-483.
WOLFF, P. M. DE (1974). *Acta Cryst.* **A30**, 777-785.
WOLFF, P. M. DE, JANSSEN, T. & JANNER, A. (1981). *Acta Cryst.* **A37**, 625-636.
YAMAMOTO, A. (1980). *Phys. Rev. B*, **22**, 373-379.
YAMAMOTO, A. (1982). *Acta Cryst.* **A38**, 87-92.
YAMAMOTO, A. (1983). *Phys. Rev. B*, **27**, 7823-7825.

Acta Cryst. (1988). **A44**, 239-243

Small-Single-Crystal Diffractometry with Monochromated Synchrotron Radiation – the Wavelength-Dispersion Minimum Condition for Bragg Reflection Profile Measurement

BY A. MCL. MATHIESON

Chemistry Department, La Trobe University, Bundoora, Victoria, Australia 3083

(*Received* 1 *July* 1987; *accepted* 20 *October* 1987)

Abstract

The interaction of a synchrotron beam incident on a 'perfect' monochromator crystal, M, and then on a small single crystal, c, is examined and the resultant 2D shape in $\Delta\omega$, $\Delta 2\theta$ space of Bragg reflections from c is deduced. This allows (a) identification of the components intrinsic to M which contribute to the shape, namely its effective aperture and angular bandpass, and (b) prediction of the change of shape with θ_c. Projection of the 2D shape onto the $\Delta\omega$ axis yields the corresponding 1D 'counter' profile and shows that, for Gaussian-like components, the full width at half maximum (FWHM) of the profile is $[p^2+q^2(t-t_{\min})^2]^{1/2}$ where p and q are constants, $t=\tan\theta_c/\tan\theta_M$ and $t_{\min}$ corresponds to the minimum dispersion condition. It is suggested that, for similar conditions, the relationship determining scan range should be of a similar functional form rather than the conventional linear relationship.

Introduction

The angular divergences involved in synchrotron beam lines are considerably smaller than those associated with conventional X-ray sources. Indeed, one might be inclined to conclude, following the discussion in Willis (1960), relating to divergence $(a)\sim 0°$, that this near-parallelism could lead to the minimum dispersion condition for the 'counter' profile in the synchrotron-radiation (SR) case occurring nearer $t=-2$ than $t=-1$, t being $\tan\theta_c/\tan\theta_M$. However, as we will show, this does not appear to be the case.

Nevertheless, the smaller divergence does provide a greater possibility, in single-crystal diffractometry on a beam line, of deriving quantitative estimates of the reflectivity curves of specimen crystals which, for 'imperfect' crystals, is closely allied to the mosaic spread, Mathieson (1984a). Even so, the influence of components intrinsic to the system, such as the effective aperture (illuminated length) of the monochromator crystal and the corresponding angular bandpass, cannot be ignored. It is therefore useful to establish their influence on the shape of Bragg reflections, especially in respect of change with scattering angle of the specimen crystal. This information can then be used to derive realistic estimates of reflectivity curves by deconvolution of experimental data, *cf.* Schneider (1977).

For the combination of a 'perfect' monochromator crystal, M, and a specimen crystal, c, of nominally zero mosaic spread, the 2D shape in $\Delta\omega$, $\Delta 2\theta^{(0)}$ space (for terminology, see Mathieson, 1983) of the Bragg reflection from c is deduced and its change with θ_c is studied. The corresponding change in the more generally used 1D 'counter' profile is then derived and compared with published data.

From the conclusions concerning counter profile width, observations are offered on a form of relationship, different from the accepted linear one, which would appear to be appropriate to determine scan range for small-crystal measurement on synchrotron sources. Use of this relationship should ensure uniform rather than variable truncation, *e.g.* Denne (1977), and hence estimates of integrated intensity which are consistent from reflection to reflection.

0108-7673/88/030239-05$03.00

The monochromator/specimen crystal interaction

In a synchrotron beam line, the source aperture, effectively of outer dimensions *ca* 1-2 mm (Brookhaven National Laboratory, 1985), is at a distance of decametres from a monochromator system consisting of 'perfect' crystals (usually two in 'parallel' configuration) and sometimes including a cylindrical or toroidal mirror. This combination results in a beam convergent on the small-single-crystal specimen and comprising a range of wavelength, which, although small from the viewpoint of a laboratory set-up, is not insignificant in the context of experiments with SR. This configuration can, for our discussion, be replaced by the simpler arrangement shown in Fig. 1, consisting of an extended-face monochromator 'perfect' crystal, M, *i.e.* with 'zero' mosaic spread but still involving intrinsic Darwin angular width. The central beam from the source, of wavelength λ_0, diffracts at the Bragg angle θ_M from the central point M_0 on the surface of M, towards the specimen crystal, c (considered effectively as a point). Crystal c is also considered for present purposes to be 'perfect'. Associated with any point on the monochromator surface, such as the outer-limit point, M_+, is a potential 'acceptor fan', of wavelengths adjacent to λ_0, the potential range, in this case, being shown in the insert in Fig. 1. Each ray of the 'acceptor fan' proceeds after diffraction from M_+ along the line M_+c at an angle $\theta_M + \Delta\theta_M$ to the surface of M. As Fig. 1 shows, each ray of the 'acceptor fan' is associated with a specific wavelength but the range of wavelength is limited by the Darwin width of M and the intensity passed on depends on whether the ray 'sees' the source. The ray M_+c is therefore associated with a small band of wavelengths. Since we are dealing here only with the interaction at the surface of M, *i.e.* no penetration of M, the angle $\Delta\theta_M$ is determined entirely by the position of the point M_+. To establish a wavelength reference, let us identify the deviant wavelength of that component of the potential 'acceptor fan' associated with the *symmetrical reflection* at M_+ with the scattering angle $2\theta_M + 2\Delta\theta_M$ as $\Delta\lambda_{+2}$, see Fig. 1 and inset. This gives the general relationship

$$\Delta\theta_M = (\Delta\lambda_{+2}/\lambda_0)\tan\theta_M. \qquad (1)$$

Note that $\Delta\theta_M$ is a fixed value for each point on M. Depending on whether it 'sees' the source, $\Delta\lambda_{+2}$ may be inside or outside the operational wavelength determined by the actual experimental arrangement.

Following the terminology of Allison & Williams (1930), diffraction from M establishes the + scattering direction so that the subsequent scattering from c in the region of the so-called 'parallel' condition, which is our main concern, is in the − scattering direction; to avoid the confusion of increasing negative angles, we identify $\Delta\omega_c$ and $\Delta 2\theta_c^{(0)}$ in this region by (−). $(-)\Delta\omega_c$ corresponds to the fractional displacement of the specimen-crystal rotation in the region of the particular Bragg reflection under consideration while $(-)\Delta 2\theta_c^{(0)}$ corresponds to the fractional displacement across detector space. Note that 2θ identifies the detector axis and does not correspond to $2\times\theta$. The superscript to 2θ indicates the scan mode linking the detector axis and the specimen-crystal axis, $s = \Delta 2\theta/\Delta\omega$, see Mathieson (1983); $s = 0$ means the detector is stationary (the so-called ω-scan mode). In the region of a Bragg reflection, Fig. 1, the appropriate general relationship (Mathieson, 1985*a*) is given by

$$(-)\Delta\omega_c = -\Delta\theta_c + \Delta\theta_M. \qquad (2)$$

As shown above, the beam M_+c consists of a band of wavelengths, so (2) may also be formulated (dropping the subscript c) in terms of wavelength dispersion as

$$(-)\Delta\omega = (\Delta\lambda_i/\lambda_0)\tan\theta_c + (\Delta\lambda_{+2}/\lambda_0)\tan\theta_M, \qquad (3)$$

where $\Delta\lambda_{+2}$ is fixed (as the symmetrical reflection from M) and $\Delta\lambda_i$ is variable, *i.e.* it can correspond to any wavelength within the 'acceptor fan'. This can be normalized in terms of $t = \tan\theta_c/\tan\theta_M$ as in

$$(-)\Delta\omega = (\Delta\lambda_{+2}/\lambda_0)\tan\theta_M[(\Delta\lambda_i/\Delta\lambda_{+2})t + 1] \qquad (4a)$$

$$= k'[(\Delta\lambda_i/\Delta\lambda_{+2})t + 1], \qquad (4b)$$

where $k' = (\Delta\lambda_{+2}/\lambda_0)\tan\theta_M$. For M_0, $\Delta\lambda_{+2} = 0$ and (3) and (4) simplify to $(-)\Delta\omega = (\Delta\lambda_i/\lambda_0)\tan\theta_c$.

For $\Delta 2\theta^{(0)}$, the relationship corresponding to (4*b*) is therefore

$$(-)\Delta 2\theta^{(0)} = k'[2(\Delta\lambda_i/\Delta\lambda_{+2})t + 1]. \qquad (5)$$

We treat here only $\Delta\omega$, $\Delta 2\theta^{(0)}$ space, *i.e.* the ω-scan mode, other scan modes can be readily derived, see Mathieson (1983).

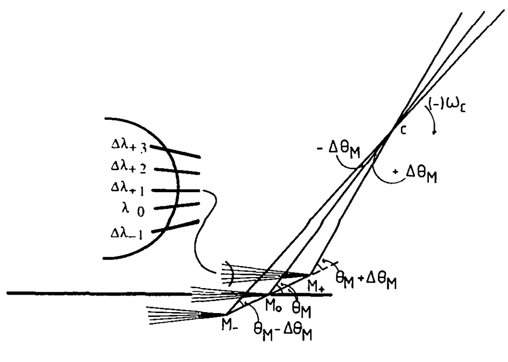

Fig. 1. Interaction of the beam incident on a monochromator crystal, M, and diffracted to the specimen crystal, c. For each point on M, an 'acceptor fan' of beams whose wavelength deviation from λ_0 is designated as $\Delta\lambda_{+n}$ is diffracted and passes to c. M_+ is a typical point, and the beam M_+c is at an angle $\theta_M + \Delta\theta_M$ to the surface of M. M_0 is the central point of M and the corresponding angle is θ_M. The region of scattering which concerns us is the 'parallel' region, $(-)\omega_c$.

The resultant shape in $\Delta\omega$, $\Delta 2\theta^{(0)}$ space

The change of the wavelength band associated with any point on M and its dispersion as θ_c changes and how these factors determine the shape of the Bragg reflection in diffraction space can be appreciated most readily in diagrammatic form in $\Delta\omega, \Delta 2\theta^{(0)}$ space, Fig. 2.

In Fig. 2, the origin, O, corresponds to the central beam from M_0 through c for wavelength λ_0. O' corresponds to the λ_0 component of the beam from M_+ through c while O'' is that for M_-. The line $O'OO''$ is at 45° to the $\Delta\omega$ and $\Delta 2\theta^{(0)}$ axes. Note that for $\theta_c = 0°$, the dispersion of c is zero, so all components of the wavelength band passed by M_+ coincide at O', similarly those for M_0 at O and those for M_- at O''. Hence the shape of the Bragg reflection for this condition, including the wavelength bands dispersed by the monochromator M, is a straight line at 45° to the two axes, see Mathieson (1985*b*).

Again from Fig. 2, as θ_c increases and moves into the 'parallel' region, *i.e.* as $(-)\Delta\omega_c$ increases (Fig. 1), the wavelength components from M_+ will be dispersed along the line $Z'_+O'Z'_-$ while those from M_- will be dispersed along the line $Z''_-O''Z''_+$ and those from M_0 along Z_-OZ_+. In detail, any wavelength associated with M_+ which is positive deviant from λ_0 is displaced along $O'Z'_-$ while negative deviant components are displaced along $O'Z'_+$. The λ_0 component remains undisplaced at O'. For M_-, positive deviant components are displaced along $O''Z''_+$ while negative deviant components are displaced along $O''Z''_-$, the λ_0 component remaining undisplaced at O''. For M_0, positive deviant components are displaced along OZ_+ and negative deviant components along OZ_-.

From the form of (4*b*) and (5), the lines $Z'_+O'Z'_-$, $Z''_-O''Z''_+$ and Z_-OZ_+ are scaled linearly in t relative to the line origins, O', O'' and O respectively. Thus, in respect of the reference deviant wavelength $\Delta\lambda_{+2}$, A' (A'') corresponds to $t = -0{\cdot}5$ and B' (B'') to $t = -1{\cdot}0$ (see Mathieson, 1985*a*). For other deviant wavelengths, $\Delta\lambda_i$, the linear scale changes proportionally.

The disposition of any wavelength band in $\Delta\omega$, $\Delta 2\theta^{(0)}$ space can be determined for any nominated value of t. For illustration, consider a case for a value of t (say) *circa* $-0{\cdot}9$ where the wavelength band from M_+ corresponds to $\Delta\lambda_{+1{\cdot}2}$ to $\Delta\lambda_{+2}$, *i.e.* points P and Q respectively on $O'Z'_-$. The corresponding band for M_- will be $\Delta\lambda_{-2}$ to $\Delta\lambda_{-1{\cdot}2}$, *i.e.* points S and R respectively on $O''Z''_-$, while, for M_0, it will be $\Delta\lambda_{-0{\cdot}4}$ to $\Delta\lambda_{+0{\cdot}4}$, *i.e.* points N_- and N_+ respectively. These combined conditions correspond to the parallelogram *PQRS* in Fig. 2.

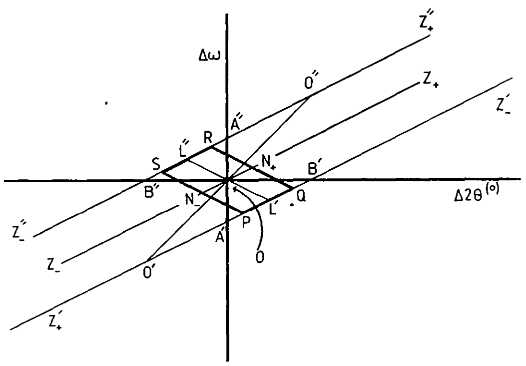

Fig. 2. *PQRS* is the outer-limit shape of a typical Bragg reflection in $\Delta\omega, \Delta 2\theta^{(0)}$ space for a value of t ($= \tan\theta_c/\tan\theta_M$) *circa* $-0{\cdot}9$. The origin of $\Delta\omega$, $\Delta 2\theta^{(0)}$ space is O and corresponds to the central beam from M_0 through c for $\theta_c = 0°$, while O' (O'') corresponds to the equivalent beam from M_+ (M_-) (outer limits of M). So the line $O'OO''$ corresponds to the shape for $\theta_c = 0°$, *i.e.* a straight line at 45° to the $\Delta\omega$ and $\Delta 2\theta^{(0)}$ axes. With increase of θ_c into the 'parallel' region, Fig. 1, any wavelength associated with M_+ which is positive deviant from λ_0 is displaced along $O'Z'_-$ while negative deviant wavelengths are displaced along $O'Z'_+$. Similar relationships hold for M_- and for M_0 along $Z''_+O''Z''_-$ and Z_+OZ_-. Thus, for the reference deviant wavelength $\Delta\lambda_{+2}$, A' (A'') corresponds to $t = -0{\cdot}5$ and B' (B'') to $t = -1{\cdot}0$. *PQRS* illustrates the situation for $t \sim 0{\cdot}9$ and a small wavelength band passed by M. *PQ* corresponds to the wavelength band $\Delta\lambda_{+1{\cdot}2}$ to $\Delta\lambda_{+2}$, *SR* to $\Delta\lambda_{-2}$ to $\Delta\lambda_{-1{\cdot}2}$ while N_-N_+ corresponds to $\Delta\lambda_{-0{\cdot}4}$ to $\Delta\lambda_{+0{\cdot}4}$. The composition of the deviant wavelength band changes from *PQ* to *RS* but the band size is constant.

The outer-limit shape, *PQRS*, is therefore determined by two components. The first is due to the monochromator-system aperture (or illuminated length on M) and how this is modified by the interaction of the dispersion of the specimen crystal. This component lies within the limit lines $Z'_+O'Z'_-$ and $Z''_-O''Z''_+$ and corresponds to the centre line of the wavelength bands, namely $L'OL''$. The second is due to the equivalent angular size of the wavelength bands passed by the monochromator system and how these are dispersed by c. This corresponds to N_-ON_+; and depends, *inter alia*, on the 'Darwin width' of M.

These two components both vary with t but in different ways. Thus the intensity distribution within *PQRS* will correspond to the multiplication of the two distributions, one parallel to $L'OL''$ and the other parallel to N_-ON_+. With change of t, the first distribution rotates about O starting from the line $O'OO''$, moving to $A'OA''$, then through $L'OL''$ to $B'OB''$ and so on, its limits always following the lines $Z'_+O'Z'_-$ and $Z''_-O''Z''_+$. The second distribution starts from zero dimension at $O'OO''$ for $t = 0$ and, with increase of t, displaces along the outer-limit lines while increasing its width proportionally with t. So the shape of a Bragg reflection both rotates (first component) and expands (second component) with increase in t (and hence in θ_c). It should be noted that, although the wavelength band size remains constant from *PQ* to *RS*, its wavelength composition changes steadily. For more than two components, *e.g.* if the contribution due to the mosaic spread of c has to be included, convolution is involved in determining the distribution within the outer-limit box shape.

Projection of the 2D shape on $\Delta\omega$ – the 1D 'counter' profile

The conventional 1D 'counter' profile is determined by use of a relatively large aperture in front of the detector and corresponds to projection of the 2D shape onto the $\Delta\omega$ axis, Mathieson & Stevenson (1986). It may also be derived by convolution of the projections on $\Delta\omega$ of the individual components, *cf.* Fig. 6 in Mathieson (1984*a*). If, for illustration, we assume that the distributions corresponding to the two components treated in the previous section are Gaussian, then we can identify the form of their variation with t in terms of their FWHM.

From the last section, one can see that, for the first component, the following relationship holds

$$\Delta\omega = a(-1 + l't), \qquad (6)$$

where a is the FWHM of the monochromator aperture distribution at $t = 0$ (which can be determined in practice by replacing the specimen crystal by a small pinhole aperture and scanning in $\Delta 2\theta^{(0)}$ with a fine slit in front of the detector). In terms of the example above, l' corresponds to the ratio of the median deviant wavelength to the deviant wavelength for the symmetrical reflection, *i.e.* $(\Delta\lambda_{+1\cdot6}/\Delta\lambda_{+2})$, and the zero-dispersion condition will be at $l't_{\min} = 1$ or $t_{\min} = 1/l'$. So, in this example, *for this component alone*, the zero-dispersion condition would be at $t = 2/1{\cdot}6 = 1{\cdot}25$, not $1{\cdot}0$.

The second component will correspond to the projection of the wavelength band so the form of the FWHM, if Gaussian, will be

$$\Delta\omega = l''t, \qquad (7)$$

where l'', in the example above, will correspond to the size of the (constant) wavelength band, *i.e.* $(\Delta\lambda_{+2} - \Delta\lambda_{+1\cdot2})/\lambda_0$.

When convoluted together, this leads to a FWHM

$$\Delta\omega = \{[a(1 - l't)]^2 + [l''t]^2\}^{1/2} \qquad (8)$$

and, in this case, $t_{\min} = 1/[l' + (l'')^2/(a^2 l')]$.

Alternatively, if one is not concerned about the specific physical meaning of the parameters in (8), the FWHM relationship can be formulated in general terms as

$$\Delta\omega = [p^2 + q^2(t - t_{\min})^2]^{1/2}, \qquad (9)$$

$t_{\min}$ corresponding to the value of t where the wavelength dispersion is at a minimum.

To demonstrate the application of such a relationship, we can use some recent data of Höche, Schulz, Weber, Belzner, Wolf & Wulf (1986) derived from measurements on an Si 'perfect'-crystal specimen so that the intrinsic influence of specimen mosaic spread is avoided or at least minimized. In Fig. 3, the data on profile widths, including the estimates of deviations, plotted *vs* θ_c in Fig. 2 of Höche *et al.* (1986) have been replotted *vs* t. A little trial and error yields a close fit, the full line in the figure, corresponding to $p = 3{\cdot}075(\times 0{\cdot}003°)$, $q = 1{\cdot}278(\times 0{\cdot}003°)$ and $t_{\min} = -1{\cdot}2$.

Scan range and profile size

Where the distributions for the individual components each consist of a single peak then a relationship of the type in (8) or (9) should be applicable to the change of the combined profile shape with t. When this situation holds, a similar form of relationship, scaled by an appropriate constant, should be applicable for the setting of *scan range* since consistently-truncated measurement of integrated intensity from reflection to reflection would then hold.

This constitutes a slightly different procedure for establishing scan range from the conventional linear relationship, $a + b \tan\theta_c$, or more appropriately in this case, $a' + b'|t - t_{\min}|$. Obviously, for $|t| \gg t_{\min}$, the two procedures would be largely indistinguishable in operational terms but where a (a') and b (b') are of similar magnitude they would deviate significantly.

Where a component involves two (or more) peaks, the profile (and scan-range) relationship will require modification because the separation between the peaks will have to be included as a linear contribution. For most synchrotron circumstances, however, the components consist of single peaks.

Höche, Schulz, Weber, Belzner, Wolf & Wulf (1986) have proposed a similar relationship for profile width but have referred it to a minimum at $\theta_c = 0°$, which corresponds to $t = 0$.

Discussion

The formulae for profile width and scan range in (8) and (9) are based on Gaussian shapes for the components. However, it should be stressed that it is only by experimental examination in $\Delta\omega$, $\Delta 2\theta^{(s)}$ space of

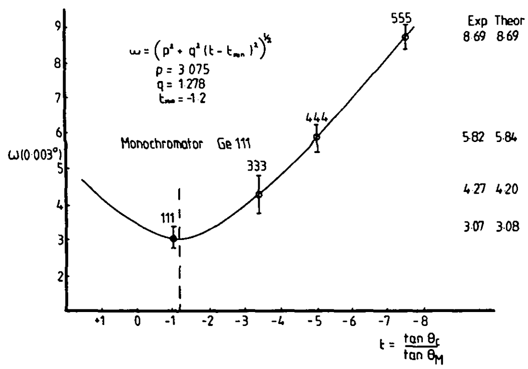

Fig. 3. Plot of the profile FWHM *vs* t. The data are derived from Höche *et al.* (1986). The continuous line represents the relationship $\omega = [p^2 + q^2(t - t_{\min})^2]^{1/2}$ with $p = 3{\cdot}075(\times 0{\cdot}003°)$, $q = 1{\cdot}278(\times 0{\cdot}003°)$ and $t_{\min} = -1{\cdot}2$.

at least a selection of Bragg reflections over the working range of θ_c that one can identify and determine the actual distributions corresponding to the various components. This information is necessary for one to be reasonably certain concerning the expected changes in 1D profile shape and the more tricky question of where to set the limits for the scan range.

To establish the estimates used for the 'profile' size or scan range, it would be advisable to carry out selected data measurement not only in the negative t region but at least part way into the positive t ('anti-parallel') region in order to establish the proper functional form of the curve, *cf.* Fig. 3. The importance of $t_{\min}$ as a reference point, equivalent to $\theta_c = 0°$ in the non-monochromator situation, should be noted. The location of $t_{\min}$ is determined by the range of the 'acceptor' fan and the effective size of the source.

The value of $t_{\min}$ for 'film' profile measurement, *i.e.* in the region of $A'OA''$ in Fig. 2 (Mathieson & Stevenson, 1986), whether by the use of film or a position-sensitive detector is of course different from $t_{\min}$ for 'counter' profiles which is in the region of $B'OB''$ since the former is in the region of t approximately half that of the latter. As shown above, neither require to be at $t = -0{\cdot}5$ or $-1{\cdot}0$ exactly.

The significance of $t_{\min}$ as a reference point for profile measurement has been stressed. It should also be noted that the wavelength dispersion *inverts* at this point, a feature of concern only if the wavelength band distribution is not symmetrical - which may be the case for monochromatized synchrotron radiation because of the role of the intensity distribution under dynamical conditions.

As mentioned at the beginning, the effect of mosaic spread of the specimen crystal has not been included specifically in the present treatment. In the case of a 1D profile, the contribution from the mosaic spread of c would be included in p in (9). Hence, in respect even of the data presented by Höche *et al.* (1986), the Darwin width of the specimen 'perfect' crystal (and its physical dimension) would make a contribution. From Fig. 3 of Höche *et al.*, the contribution from the physical dimension of the specimen crystal of *ca* 100 μm appears not to be gross. In any case, the only way in which one could resolve these matters would be by 2D $\Delta\omega$, $\Delta 2\theta^{(0)}$ measurements and identification of the relevant loci, see Mathieson (1982). With a scan mode other than ω scan, the locus in 2D space changes relative to the $\Delta\omega$ axis.

As mentioned in the *Introduction*, one might expect from consideration of Fig. 1 that, with the small divergence of the synchrotron beam, the beams parallel to the central beam, such as $\Delta\lambda_{+1}$ in relation to M_+, would be dominant and that therefore the minimum dispersion would occur near $t = 2$ $(1/l' = \Delta\lambda_{+2}/\Delta\lambda_{+1})$, *cf.* Willis (1960). However, it appears that, although the divergence and the 'Darwin width' of the monochromator system are both small, nevertheless there is sufficient relaxation from parallelism to allow $t_{\min}$ to come closer to 1.

It should be noted from above that, for our present purposes, we have ignored the contribution associated with the physical size of the specimen crystal. Its functional dependence on θ_c may be quite complex, see Mathieson (1984*b*), also McIntyre (private communication).

An opportunity to gain experience concerning synchrotron X-radiation was provided by a grant from the Australian Government Department of Science under the US/Australia Science and Technology Agreement. This made possible an exchange visit (July/September 1986) with Dr B. P. Schoenborn of the Biology Department, Brookhaven National Laboratory, Upton, NY 11973, USA, to work on beamline X-12C of the National Synchrotron Light Source (NSLS). His support and cooperation were greatly appreciated. The author also thanks Dr A. Kvick of the Chemistry Department, BNL, for demonstrating the capability of the single-crystal diffractometer facility of that Department on beamline X-13B of the NSLS to derive the $\Delta\omega$, $\Delta 2\theta^{(0)}$ distribution of a Bragg reflection.

Thanks are due to Professor H. Schulz and to Dr B. T. M. Willis for correspondence concerning details in their respective papers. Also to Drs M. F. Mackay and A. W. Stevenson and to Dr J. K. Mackenzie in particular for discussion and critical comments on the present test. And to an anonymous referee for valuable critical comments.

References

ALLISON, S. K. & WILLIAMS, J. H. (1930). *Phys. Rev.* **35**, 149-154.

BROOKHAVEN NATIONAL LABORATORY (1985). National Synchrotron Light Source, Annual Report 1985 (Document BNL-51947), pp. 167, 230, 276. Brookhaven National Laboratory, New York, USA.

DENNE, W. A. (1977). *Acta Cryst.* **A33**, 987-992.

HÖCHE, H. R., SCHULZ, H., WEBER, H.-P., BELZNER, A., WOLF, A. & WULF, R. (1986). *Acta Cryst.* **A42**, 106-110.

MATHIESON, A. McL. (1982). *Acta Cryst.* **A38**, 378-387.

MATHIESON, A. McL. (1983). *J. Appl. Cryst.* **16**, 257-258.

MATHIESON, A. McL. (1984*a*). *Acta Cryst.* **A40**, 355-363.

MATHIESON, A. McL. (1984*b*). *J. Appl. Cryst.* **17**, 207-209.

MATHIESON, A. McL. (1985*a*). *Acta Cryst.* **A41**, 309-316.

MATHIESON, A. McL. (1985*b*). *Acta Cryst.* **A41**, 603-605.

MATHIESON, A. McL. & STEVENSON, A. W. (1986). *Acta Cryst.* **A42**, 435-441.

SCHNEIDER, J. R. (1977). *Acta Cryst.* **A33**, 235-243.

WILLIS, B. T. M. (1960). *Acta Cryst.* **13**, 763-766.